Journal of Thermal Science Vol.27, No.3 (2018) 259–269

https://doi.org/10.1007/s11630-018-1007-2 **Article ID:1003-2169(2018)03-0259-11**

Compressor and Turbine Multidisciplinary Design for Highly Efficient Micro-gas Turbine

BARSI Dario[1], PERRONE Andrea[1], QU Yonglei[2], RATTO Luca[1], RICCI Gianluca[1], SERGEEV Vitaliy[3], ZUNINO Pietro[1*]

1. Department of Mechanical, Energy, Management and Transport Engineering, Università degli Studi di Genova, Genova, Via Montallegro 1, I-16145, Italy

2. Faculty of Power and Energy Engineering, Harbin Engineering University, Harbin, 150001, China

3. Institute of Energy and Transport Systems, "Peter the Great" St. Petersburg Polytechnic University, Polytechnicheskaya str. 29, Saint Petersburg, 195251, Russia

Abstract: Multidisciplinary design optimization (MDO) is widely employed to enhance turbomachinery components efficiency. The aim of this work is to describe a complete tool for the aero-mechanical design of a radial inflow turbine and a centrifugal compressor. The high rotational speed of such machines and the high exhaust gas temperature (only for the turbine) expose blades to really high stresses and therefore the aerodynamics design has to be coupled with the mechanical one through an integrated procedure. The described approach employs a fully 3D Reynolds Averaged Navier-Stokes (RANS) solver for the aerodynamics and an open source Finite Element Analysis (FEA) solver for the mechanical integrity assessment.

Due to the high computational cost of both these two solvers, a meta model, such as an artificial neural network (ANN), is used to speed up the optimization design process. The interaction between two codes, the mesh generation and the post processing of the results are achieved via in-house developed scripting modules. The obtained results are widely presented and discussed.

Keywords: Micro-gas turbine; Multidisciplinary Optimization; Centrifugal Compressor; Centripetal Turbine

1. Introduction

Micro-gas turbines used in cogeneration power plants represent a promising technical solution for distributed combined production of electricity and heat, especially due to their low emissions and fuel flexibility. Even though the global energy efficiency of micro-gas turbines is usually high, due to the use of waste heat for cogeneration, the electrical efficiency is lower than other competing technologies such as reciprocating internal combustion engines. As a consequence, an effort should be made to enhance its performance. This target can be obtained by increasing the turbine inlet temperature in order to improve Brayton cycle thermodynamic efficiency or by means of an integrated and optimized design of micro-turbine components (centrifugal compressor, radial inflow turbine, recuperator, combustor, etc.). Both these approaches are subject of researches even though they have different impact on machine manufacturing process. The first approach requires the use of advanced materials for the hot gas path components, such as ceramic turbine impeller and casing and nickel based super-alloy recupe-

Received: January 15, 2018 Corresponding author: ZUNINO Pietro, Professor E-mail: pietro.zunino@unige.it

Nomenclature

ANN	Multi Layer Perceptron Artificial Neural Network	W	Weight term for penalty function [*dimensionless*]
a	Constant variable	w	Relative velocity [m/s]
b	Channel width [m]	y^+	Dimensionless wall distance [*dimensionless*]
c	Absolute velocity [m/s]	**Greek**	
CFD	Computational Fluid Dynamics	α	Absolute flow angle [*deg*]
c_p	Pressure coefficient [*dimensionless*]	β	Pressure ratio [*dimensionless*]
D	Diameter [m]	η	Efficiency [*dimensionless*]
DoE	Design of Experiments	ϑ	Tangential coordinate [*deg*]
EO	Engine Order	σ	Stress [MPa]
FEA	Finite Element Analysis	**Subscript & superscript**	
F	Frequency [Hz]	0	Inlet section
GA	Genetic algorithm	1	Interstage section
L	Excitation harmonic number [*dimensionless*]	2	Outlet section
LE	Leading Edge	*Aero*	Aerodynamic
$L_{1\text{-}2}$	Specific work [J/kg]	*all*	Allowable
M	Nodal diameter [*dimensionless*]	*eigfr*	Eigenfrequency
m	Meridional coordinate [m]	*exc*	Exciting
$\dot{m}$	Mass flow rate [kg/s]	*Freq_high*	High frequency
Ma	Mach number [*dimensionless*]	*Freq low*	Low frequency
MDO	Multidisciplinary Design Optimization	i	Generic index
N_{rotor}	Number of rotor blades	*is*	Isentropic
N_{vane}	Number of vane blades	*MAX*	Maximum
n	Shaft speed [r/min]	*MIN*	Minimum
n_s	Specific speed based on machine outlet density [*radians*]	*NPF*	Relative to nozzle passing frequency
$\bar{n}_s$	Specific speed based on impeller inlet density [*radians*]	*OUT*	Outlet
P	Penalty function	r	Relative
RANS	Reynolds Averaged Navier Stokes Equations	*ROT*	Rotation
SF	Safety Factor [*dimensionless*]	*Stress*	Referred to stress analysis
T	Temperature [K]	*Struct*	Structural
TE	Trailing Edge	*t-t*	Total to total
TIT	Turbine inlet total temperature [K]	y	Yielding
u	Peripheral speed [m/s]		

rator, since cooling techniques, such as those used in larger heavy duty gas turbines, are hardly implementable with radial turbomachines. On the contrary, components redesign with advanced optimization techniques enables to keep the current technology for component manufacturing leading, therefore, to significant performance enhancement [1].

Summarizing, the key parameters of the gas turbine cycle determining efficiency are:

- Cycle pressure ratio;
- Turbine inlet temperature (*TIT*);
- Turbomachinery component efficiencies.

Turbomachinery efficiency should be always maximized. However, for power lower than 1 MW and mass flow rate roughly lower than 10 kg/s, radial turbomachinery are used instead of axial ones. Centripetal turbines are more compact and less expensive than axial ones, but with the present level of manufacturing technology, cannot be cooled. Therefore, nowadays, the maximum turbine inlet temperature depends only on the material and

not on the cooling technology. Turbine inlet temperature is fixed and if ceramic material is not yet employed, a *TIT* of 950°C is the upper limit for nickel based super alloys.

As a consequence of the limited turbine inlet temperature, regeneration is necessary for reaching cycle efficiency level of about 30%, with pressure ratios compatible with single stage radial turbomachines. On the other hand, use of regeneration is made acceptable due to power lower than 1 MW. Also for the recuperated cycle, efficiency depends on pressure ratio, turbine entry temperature, turbomachinery efficiencies as for the simple Brayton cycle and further more on the recuperator effectiveness. For the recuperated cycle, best cycle efficiencies are obtained at moderate cycle pressure ratios of about 4 to 5. Pressure ratios up to 6 are compatible for single stage centrifugal compressors and centripetal turbines. The research team of the Laboratory of Aerodynamics, Combustion and Turbomachinery of University of Genova has a long standing experience in the study, development and testing of gas turbine components for energy generation and propulsion. Since some years the research team is active in the multidisciplinary optimization design (MDO) of key components of micro gas turbines for energy cogeneration [3]. The present paper summarizes the results of compressor and turbine design activity.

2. Efficiency enhancement

As discussed in the introduction, the optimized design of components enables to reach significant efficiency improvement with a negligible impact on the technology, on the manufacturing process and on the materials to be employed. Fig. 1 shows the impact of *TIT* increase and component optimization on the MGT electrical efficiency. In particular, temperature values of 950 °C and 1100 °C have been considered as the representative values for, respectively, nickel based super-alloy and ceramic turbine impeller.

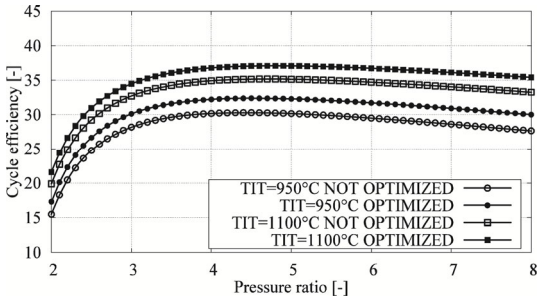

Fig. 1 Comparison of efficiency enhancement obtained by means of *TIT* increase or components optimization

An optimized and integrated design for compressor, turbine and recuperator has been considered for enhancing efficiency values from current commercial machines to state of the art for advanced applications. A way to achieve the goal of enhancing MGT efficiency is the employment of an integrated design procedure for the whole machine, considering the mutual interaction of the components, employing multidisciplinary optimization (MDO) techniques, able to satisfy on one hand the requirements of obtaining high efficiency for all MGT components, and on the other hand to guarantee the safe operation of the machine imposed by technological and mechanical integrity constraints. Advanced simulation models for mechanical analysis and assessment have to be developed, especially in the case of adoption of ceramic material for the turbine rotor. Static and dynamic analyses have to be integrated in the multidisciplinary optimization calculation cycle, but more advanced and detailed analyses will be carried out for the optimized sample. In particular, transient conditions represent a key factor for assessing the Low Cycle Fatigue (LCF) and minimizing the clearances. Moreover, a good dimensioning of bearings and lubrication and analysis of shaft operation is required, in order to avoid misestimating of mechanical efficiency or of bearings life. Related to the shaft and the bearings, another important topic is the rotor dynamic behaviour of the machine: the shaft layout strongly affects the eigenfrequencies of the system, which can occur at a speed lower than the operating one; therefore, in the start-up phase, the bearings should be able to damp the vibration amplitudes of the shaft. In turbomachines shaft layout and compliance of the bearings, i.e. their stiffness and damping, influence critical speeds and out-of-balance response of the rotor. Bearings must provide sufficient damping to operate with vibrations of acceptable amplitude in nominal conditions and, for supercritical rotors, to overcome the critical speed without damage. In addition, for fluid film bearings, instabilities generated by the fluid and its interaction with other parts (whirl, whip, hammering) must be avoided.

3. Cycle optimization

The concept design of the micro gas turbine starts from the analysis of a regenerative Brayton cycle (Fig. 2) suitable for the specific application. In the present paper, a micro turbine for cogenerate application with 100 kW of electric power output has been considered. Relating to the fluid-dynamic parameters such as components efficiencies, total pressure losses, heat transfer and insulation coefficients, several assumptions have to be considered.

These parameters have been assumed from literature component datasheets and other scientific papers and are summarized in Table 1. These values represent the state of the art of a 100 kW micro gas turbine technology available on the market. The calculations have been carried out through the open source in-house developed code GTcycle [6].

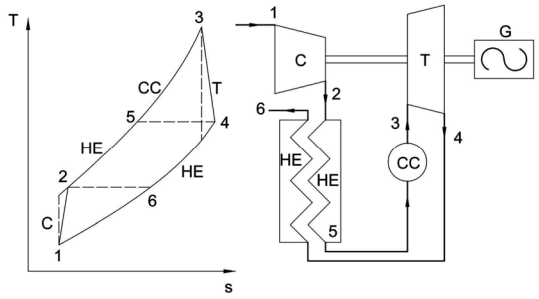

Fig. 2 Regenerative Brayton cycle

Table 1 Main cycle parameters for 100 kW micro-gas turbine

Parameters	Value
Compressor efficiency	80%
Turbine efficiency	86%
Recuperator effectiveness	84%
Pinch point temperature difference	70 °C
Combustor efficiency	95%
Generator efficiency	96%
Mechanical efficiency	99%
Compressor pressure ratio	4.4
TIT	950 °C
Recuperator hot pressure losses	100 mbar
Recuperator cold pressure losses	150 mbar
Combustor pressure losses	175 mbar
Intake pressure losses	10 mbar
Exhaust pressure losses	10 mbar
Cycle Efficiency	30%

The considered cycle has a maximum turbine inlet temperature of *TIT*=950 °C. This value is established by the maximum thermal load that can be applied to nickel based super alloys, since the blades are not cooled. For this *TIT* value, a total-to-total pressure ratio of the cycle, $\beta_{t-t\ cycle}$=4.4 has been found to maximize the Brayton-Joule thermodynamic efficiency. It results in a total-to-total pressure ratio of the turbine of $\beta_{t-t\text{turb}}$ = 3.7, once the pressure drop in the combustion chamber as well as in the exhaust duct and regenerator are considered. Finally, in order to obtain the desired net output power of the system, P = 100 *kWe*, a target mass flow rate of 0.75 kg/s has been considered. As reported in the previous table, the efficiency of the thermodynamic cycle is about 30%. This value can be improved increasing the *TIT* over the current technological limit of 950 °C due to the limit of nickel super alloys. In recent years, a great deal of effort has been devoted to research and development of innovative ceramic materials for the manufacturing of turbine impellers in order to increase turbine inlet temperature and, consequently, to enhance the global efficiency. To overcome this technological limit, advanced cooling techniques are employed both in industrial heavy duty gas turbines and aero-engines. However, there are very few applications of cooled radial impellers, mainly due to manufacturing constraints. A thorough investigation has been carried out in order to highlight the influence of each micro GT component efficiency variation on the overall cycle efficiency. Fig. 3 shows two levels of main components optimization and values are summarized in Table 2.

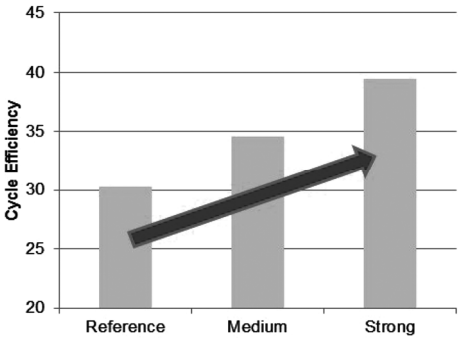

Fig. 3 Effect of components optimization on cycle efficiency

Considering compressor and turbine, results have shown that the same component efficiency increase leads to different overall cycle efficiencies. This is the consequence of the lower specific energy exchange of the compressor with respect to the turbine, with a greater influence of the latter.

Table 2 Assumed efficiency and effectiveness of components for two levels of expected optimization.

	Reference	Medium	Strong
Compressor	80%	82%	84%
Turbine	86%	88%	90%
Recuperator	84%	89%	94%

The recuperator effectiveness strongly affects the machine efficiency. Recuperator design has to be a compromise between performance improvement, size and weight constraints.

Finally, a strong optimization of the main components, preserving the same *TIT*, can lead to efficiency values up to 38%, much larger than the present state of the art. However, such level of component efficiency improvement is hardly obtainable due to the inherent small dimensions of the components.

4. Multidisciplinary optimization

The centrifugal compressor and the centripetal turbine first guess geometries, which are required by the optimization procedure, have been designed starting from a

one-dimensional preliminary approach aimed at fulfilling the design duty with the best machine efficiency, also taking into account mechanical limitations of the materials.

In this first design step, the main dimensions and blade angles have been found applying 1D equations, starting from statistical relationships and literature data to set the ranges for the main unknown design parameters.

Among others, the literature source was constituted for compressor 1D design mainly by Ref. [7] and for the turbine 1D design by Ref. [14]. For the 1D design, in house developed codes have been utilized.

5. Geometry parameterization

The commercial software Numeca/Autoblade [18] has been employed to choose a proper set of parametric curves and to identify the most appropriate geometrical topology that enables the designer to manage different geometrical shapes via a limited number of key parameters automatically defined within the optimization environment.

For achieving axial-to-radial configuration, both hub and shroud contours present the same geometrical topology: an axial line part, followed by a Bezier curve with 4 control points, to end it up with another line, radially directed.

The impeller row is made up of a main blade and a splitter blade. For main blade camber parameterization, a Bezier curve, controlled by 5 points equally distributed along the abscissa, has been employed for each of the three spanwise sections.

For half-thickness law definition, a Bezier curve with 4 control points has been employed on each spanwise section. The diffuser row is made up of straight wedge-shaped blades. They are cylindrical, unleaned and not tapered blades.

After imposing the required constraints, the compressor parametric geometrical model has 26 degrees of freedom.

For the radial turbine, the three-dimensional representation of the machine is defined by the meridional channel geometry, the stator and rotor blade camber line and thickness curves and by the definition of blade positions along the channel (Fig. 4).

Similar to compressor parameterization, Bezier curves have been used for geometry representation within the automatic optimization tool. The stator row has been defined by employing a simple Bezier for the camber line, while the thickness law is defined as thickness addition on the camber curve with a simple two-parameter law. The rotor row has been defined by employing a Bezier curve with four control points for both camber line and thickness law. In conclusion, the total number of design parameters, which will be managed by the optimization procedure for the turbine, is 22.

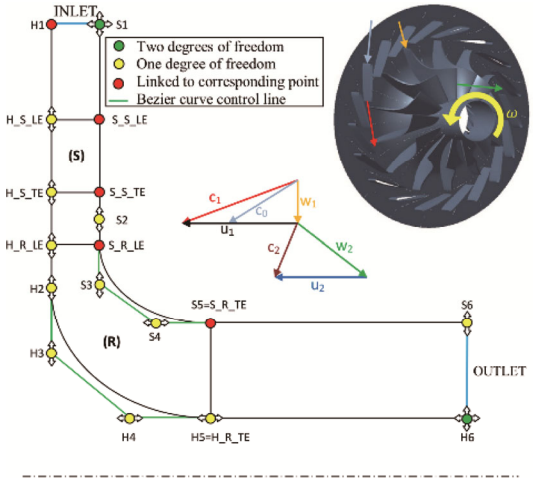

Fig. 4 Turbine geometrical parameterization and velocity standards

6. Fluid and solid mesh features, boundary conditions and FEA

The whole fluid domain has been meshed by means of Numeca/IGG Autogrid 5. A Python script that automatically manages the multirow configuration has been implemented in order to simplify the interfacing with the optimization environment. For each row involved, a multi-block hexahedral structured mesh is built. The entire mesh is made up of about 2 million and 1.5 million of cells for compressor and turbine, respectively. The CFD calculation is arranged throughout Numeca/FineTurbo and is carried out by means of Numeca/Euranus Navier-Stokes equations solver. A RANS steady approach has been used [19] and the two-equations SST (Shear Stress Transport) [20] model has been chosen for representing turbulence phenomenology. No slip boundary condition is assumed at solid walls and rotation periodicity condition is adopted to match periodic surfaces. Moreover, the interface between impeller and diffuser row is managed by mixing plane approach. The solid mesh has been created by the open source software GMSH [22], integrated in an in house developed Python procedure. The developed procedure combines the aerodynamic optimization algorithm implemented in Fine/Design 3D with CalculiX [24], a free open source FEA. Every sample analysed through CFD for evaluating its aerodynamic performance is also verified for its structural behaviour.

7. Optimization process strategy

For the database generation, due to the high number of variables involved in the optimization process, a 25X and a 15X random sampling has been chosen for compressor

and turbine, respectively. In fact, other more refined DoE techniques would lead to too expensive computational effort. 700 (for the compressor) and 350 (for the turbine) CFD calculations, chosen randomly among the available ones, have been performed as database samples. The optimization procedure is applied in order to minimize a single objective function that is composed by the sum of several dimensionless penalty terms, each of which contains a structural or aerodynamic quantity. Due to the parabolic form of each penalty term, the objective function is convex, and therefore a minimum always exists. Each parabolic penalty term has a weighting coefficient. In the centrifugal compressor optimization, six penalty terms are employed: three aerodynamic (Equation 2-4), and three structural (Equation 5-7).

$$P_{tot} = P_{\eta_{istt}} + P_{\beta_{tt}} + P_{Ma_c} + P_{stress} + P_{freq\_low} + P_{frep\_high} \tag{1}$$

$$P_{\eta_{istt}} = \begin{cases} W_{\eta_{istt}} \left(\dfrac{1-\eta_{istt}}{0.1} \right)^2 & if \quad \eta_{istt} < 1 \\ 0 & if \quad \eta_{istt} \geq 1 \end{cases} \tag{2}$$

$$P_{\beta_{tt}} = \begin{cases} W_{\beta_{tt}} \left(\dfrac{4.5-\beta_{tt}}{1} \right)^2 & if \quad \beta_{tt} < 4.5 \\ 0 & if \quad \beta_{tt} \geq 4.5 \end{cases} \tag{3}$$

$$P_{Ma_c} = \begin{cases} W_{Ma_c} \left(\dfrac{1-Ma_c}{1} \right)^2 & if \ Ma_c \geq 1 \\ 0 & if \ Ma_c < 1 \end{cases} \tag{4}$$

$$P_{stress} = \begin{cases} W_{stress} \left(\dfrac{\sigma_{\max}}{\sigma_{all}} \right)^2 & if \quad \sigma_{\max} \geq \sigma_{all} \\ 0 & if \quad \sigma_{\max} < \sigma_{all} \end{cases} \tag{5}$$

$$\sigma_{all} = \frac{\sigma_y \left(yielding \right)}{SF \left(safety \ factor \right)}$$

$$P_{freq\_low} = \begin{cases} W_{freq\_low} \left(\left| \dfrac{f_{eigfr}}{f_{exc\_low}} - 1 \right| - 0.05 \right)^2 & if \left| \dfrac{f_{eigfr}}{f_{exc\_low}} - 1 \right| \leq 0.05 \\ 0 & if \left| \dfrac{f_{eigfr}}{f_{exc\_low}} - 1 \right| > 0.05 \end{cases} \tag{6}$$

$$P_{freq\_high} = \begin{cases} W_{freq\_high} \left(\left| \dfrac{f_{eigfr}}{f_{exc\_high}} - 1 \right| - 0.05 \right)^2 & if \left| \dfrac{f_{eigfr}}{f_{exc\_high}} - 1 \right| \leq 0.05 \\ 0 & if \left| \dfrac{f_{eigfr}}{f_{exc\_high}} - 1 \right| > 0.05 \end{cases} \tag{7}$$

The objective function is composed, regarding to aerodynamic aspects, in order to maximize the total-to-total isentropic efficiency, to guarantee the design absolute total pressure ratio and an absolute subsonic flow condition at diffuser inlet. For what concerns the structural behaviour, the aim is to keep the maximum Von Mises stress in the impeller lower than the allowable stress value and to avoid the rotor resonances. For radial turbine, the objective function for the geometry optimazation process, is made up of several penalty terms:

$$P_{Aero} = P_{\dot{m}} + P_{MAX\eta_{t-t}} + \sum_{i=1}^{4} P_{MAX\alpha_{OUT,i}} + \sum_{i=1}^{4} P_{MIN\alpha_{OUT,i}} \tag{8}$$

where

$$P_{\dot{m}} = W_{\dot{m}} \left(\frac{\dot{m}_{nom} - \dot{m}}{\dot{m}_{nom}} \right)^2 \tag{9}$$

$$P_{MIN\alpha_{OUT,i}} = \begin{cases} W_{\alpha OUT,i} \left(\dfrac{\alpha_{OUTMIN,i} - \alpha_{OUT,i}}{\alpha_{OUTMIN,i}} \right) & if \quad \alpha_{OUT,i} < \alpha_{OUTMIN,i} \\ 0 & if \quad \alpha_{OUT,i} \geq \alpha_{OUTMIN,i} \end{cases} \tag{10}$$

$$P_{MAX\alpha_{OUT,i}} = \begin{cases} 0 & if \quad \alpha_{OUT,i} < \alpha_{OUTMAX,i} \\ W_{\alpha OUT,i} \left(\dfrac{\alpha_{OUTMAX,i} - \alpha_{OUT,i}}{\alpha_{OUTMAX,i}} \right) & if \quad \alpha_{OUT,i} \geq \alpha_{OUTMAX,i} \end{cases} \tag{11}$$

$$P_{MAX\eta_{t-t}} = W_{\eta_{t-t}} \left(1 - \eta_{t-t} \right)^2 \tag{12}$$

The aim of this function is to drive the optimization process to ensure a mass flow rate equal to design condition (Equation (9)), to keep the outlet tangential velocity in a desired range along spanwise direction (sampling the

values on four spanwise sections, (Equations (10)-(11)) and to maximize the overall total to total efficiency (Equation (12)). For a preliminary assessment, an allowable stress has been defined, based on yield strength, expressed as a function of temperature, according to the following expression:

$$\sigma_{all} = \frac{a_1 T^6 + a_2 T^5 + a_3 T^4 + a_4 T^3 + a_5 T^2 + a_6 T + a_7}{SF} \quad (13)$$

where SF is a safety factor and a_i is properly defined constants. Then, Von Mises stresses of each blade node have been compared to the allowable ones, and since another target is to avoid that eigenfrequencies are in the range 0.95-1.05 of the exciting frequencies, properly penalty functions, similar to the ones defined for the compressor case, have been defined. Thus, the structural analysis objective function can be obtained as the sum of the previously described terms:

$$P_{Struct} = P_{Stress} + P_{freq\_low} + P_{freq\_high} \quad (14)$$

8. Compressor results

The optimization process has reached convergence after 35 iterations. The optimized configuration is shown in this paragraph highlighting the differences with respect to the original one and the effects of the new geometrical arrangement on the aerodynamic and structural behaviour. The physical responses to the objective function imposed are therefore explained. Figure 5 shows that in the optimized configuration the impeller inlet section relative Mach number maximum value at blade tip is decreased from 1.35 to 1.2; moreover, the region characterized by relative supersonic flow has been significantly reduced.

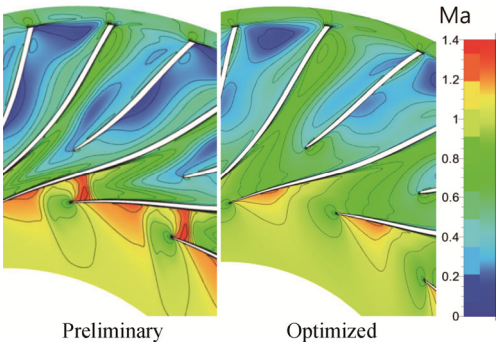

Fig. 5 Comparison of relative Mach number at 0.9 span section, impeller inlet section

Relative Mach number decreasing is mainly due to the reduction of inlet blade tip speed obtained by means of inlet radius reduction, while the inlet meridional velocity does not vary significantly since the inlet area is kept nearly constant (Fig. 6).

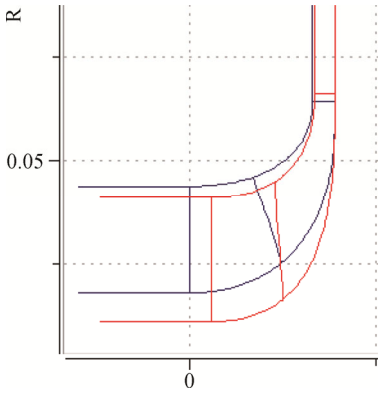

Fig. 6 Meridional section of the original (blue) and optimized (red) configuration

As concerning blade-to-blade geometrical parameters, the reduced blade thickness weakens the shock wave strength. However, it is the local null value of camber curvature at the LE that provides the greater contribution to shock wave reduction.

Figure 5 shows the improvement of flow incidence at leading edge of both main blade and splitter. The blade loading has a smoother distribution over the entire blade length. From the pressure coefficient diagrams (Fig. 7), it can be noted that in the optimized configuration the blade loading has been increased. This behaviour is consistent with the fact that similar absolute total pressure ratio is achieved in the optimized configuration with 22 instead of 24 blades.

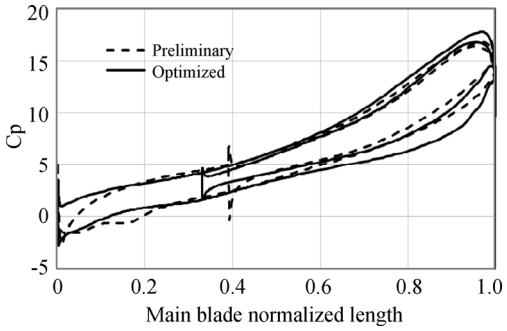

Fig. 7 Comparison of blade loading at midspan

Fig. 8 shows that in the optimized configuration the maximum value of absolute Mach number decreases. This behaviour is achieved by reducing the absolute velocity magnitude at impeller exit thanks to an increase of the backswept angle (that leads to a higher exit relative flow angle and relative velocity).

Overall, the same impeller work addition is conserved, but in the optimized configuration the same work is achieved by a larger peripheral velocity and a lower circumferential absolute velocity. That results in an unloaded impeller blade and lower absolute velocity at the diffuser inlet. Of course this has an impact on the impel-

ler structural design since the centrifugal force is increased and the impeller blade becomes more backswept.

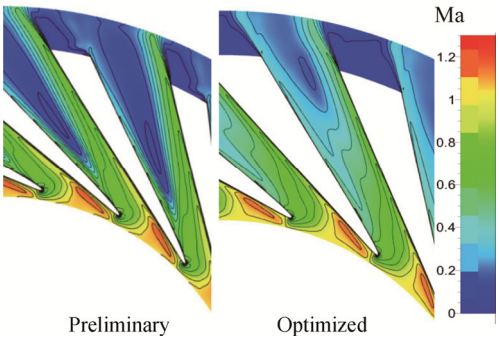

Fig. 8 Comparison of Mach number at 0.5 span section, vaned diffuser

This important aerodynamic-structural interaction shows that multidisciplinary optimization is crucial for high efficiency turbomachines.

Concerning the structural optimization, Fig. 9 shows the Von Mises stress field for preliminary and optimized configurations: the two configurations show similar maximum Von Mises stress, but in the optimized configuration the Von Mises stress map is smoother and the stress at the hub has been reduced.

In Fig. 9, the stress scale has been limited to 600 MPa for both samples.

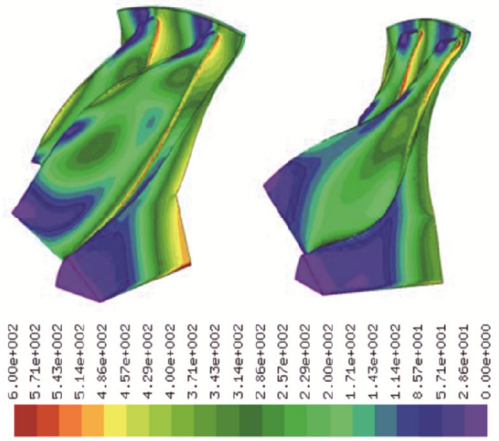

Fig. 9 Von Mises stress for the original and the optimized configuration [MPa]

The maximum Von Mises stress did not represent a limiting factor in the optimization procedure, since the use of titanium and reasoned parameters choice, which led to not excessive lean angles and blade heights, enabled to limit the overall stress distribution in the impeller. Moreover, the peak stress is concentrated in the fillet zone, in both the configurations, where some geometry simplifications have been introduced.

A complete and detailed modelling of the fillet zone will definitely reduce these stress values, which, furthermore, are concentrated in a zone where local plastic strain can be potentially accepted after a dedicated analysis for low cycle fatigue assessment. In the optimized impeller, the stress level in the blade is quite low and well balanced. Local high stresses near the rotation axis are mainly due to the constraints of the model, therefore they can be neglected. A more detailed analysis of this part could be done via axisymmetric 2D analysis but it is not the object of the present work.

Regarding the dynamic behaviour, the original configuration presents resonances with the first 4 EO and with the number of stators downstream the impeller.

In the optimized configuration, the optimization process has modified the blade design in order to meet all the dynamic assessment criteria. The original and optimized performances are summarized in Table 3.

Table 3 Original and optimized performance for centrifugal compressor

	Original	Optimized
$\dot{m}$ [kg/s]	0.74	0.74
η_{ist-t} [-]	0.80	0.84
β_{t-t} [-]	4.3	4.4
Inlet relative Mach at impeller tip [-]	1.35	1.2
Absolute Mach at diffuser inlet [-]	1.4	0.98
Stress usage factor [-]	1.2	0.95
Resonance 4EO	Yes	No
Resonance NPF	Yes	No

9. Turbine results

The optimization process has been set to 30 iterations. In order to understand the phenomena driving the optimization procedure previously discussed, the blade loading distributions in the form of static pressure coefficient c_p at hub, midspan, and tip sections are reported in Fig. 10 for both the original and the optimized geometries.

We can focus on midspan section to highlight some considerations. For the original configuration (black curves in Fig. 10), the pressure and the suction side lines intersect just behind the impeller leading edge, suggesting the occurrence of a pressure side boundary layer separation due to excessive negative incidence angle condition. The negative incidence inlet flow angle induces the formation of a recirculating flow region on the pressure side of the impeller blade. In the improved configuration, the optimization tool increases the tangential component of the absolute velocity at the rotor inlet (reducing the channel height and raising the absolute exit flow angle from the stator blade), thus reducing the negative inci-

dence at the impeller leading edge which also prevents the formation of the separated bubble characterizing the baseline configuration, as highlighted by the vector map of Fig. 13. The right incidence condition results in a better distributed blade loading as shown by the red lines of Fig. 10. As a consequence of the increased absolute tangential velocity, a higher Mach number at the stator blade trailing edge is obtained for the optimized configuration, as shown in the colour plot of Fig. 11, where the absolute (stator) and relative (rotor) Mach number distributions in the meridional plane are reported.

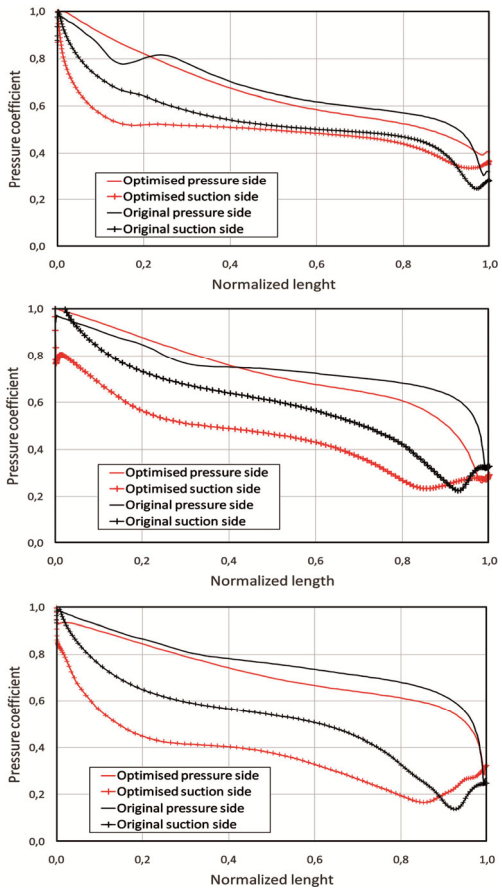

Fig. 10 Pressure coefficient diagram for rotor original and optimized configuration at hub, midspan and tip sections

Figure 11 also highlights the flow regions at the rotor exit characterized by $Ma_r > 1$. The steep pressure increase on the suction side of the blade exit shown by the pressure coefficient distribution in Fig. 10 for the baseline configuration, causes large boundary layer losses (entropy production of Fig. 12). This high relative Mach number, characterizing the original case, also sets excessive mass flow rate elaborated by the turbine as compared with the target value. Thus, the optimization procedure has acted to reduce the mass flow rate sensibly, reducing the meridional channel height (and increasing the absolute flow angle) at the stator outlet but keeping the same blade height (see Fig. 11), and decreasing the relative flow angle at the impeller outlet section. This implies an increase of the expansion in the stator and a reduction in the rotor, i.e., increasing the absolute velocity at the stator exit and reducing the relative Mach number at the rotor exit. All these effects contribute to reduce the entropy increase in the impeller, as it is made evident by the entropy fields shown in Fig. 12.

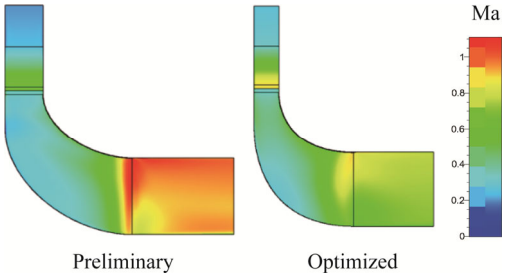

Fig. 11 Absolute and relative Mach number distributions in the meridional plane: original (left) and optimized (right) configurations

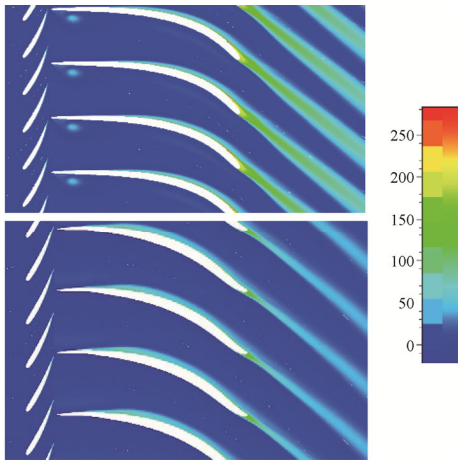

Fig. 12 Entropy field expressed in J/(kg K) for original (top) and optimized configuration (bottom) at midspan

Concerning the mechanical assessment of the turbine, as shown in Fig. 14, the original configuration presents a high stress in the midspan zone of the blade: the lean angle of the blade is very high, so the centrifugal force creates an elevated bending stress across the section. In the optimized configuration, instead the lean angle has been reduced and the higher stress is located in the fillet region, where local plastic strains are allowed, these strains, however, have to be carefully assessed through LCF analysis to predict the life of the impeller. The bending stresses on the blade, consequently, have been significantly reduced.

Fig. 15 shows the SAFE (Singh Advanced Frequency Evaluator) diagram for the original impeller, where two

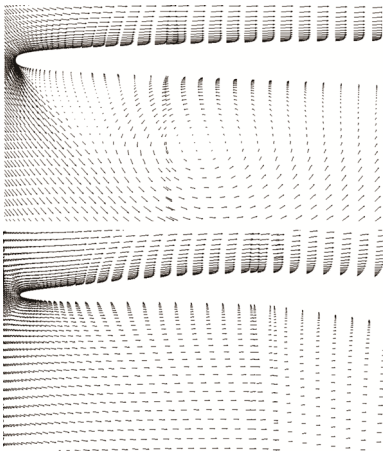

Fig. 13 Velocity vector for original (top) and optimized configuration (bottom) at midspan

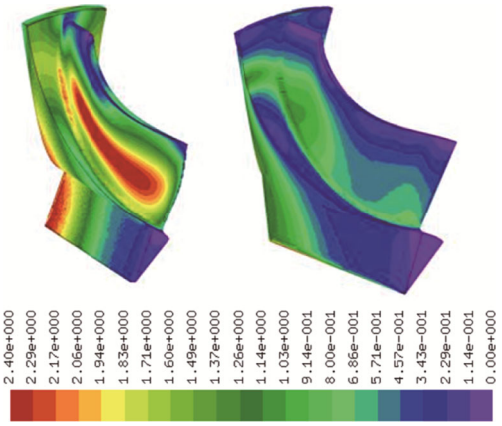

Fig. 14 Von Misesnon-dimensional stress for the original and the optimized configuration

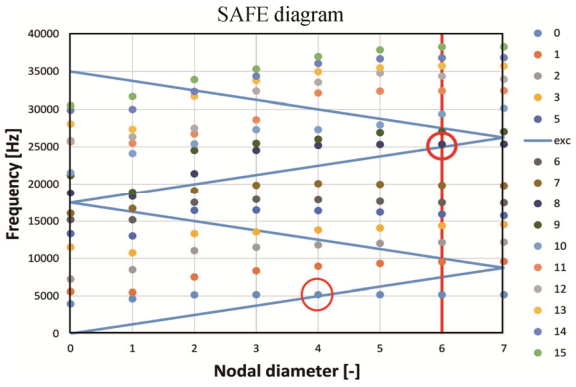

Fig. 15 SAFE diagram for the original impeller

resonances are likely to occur in the red circles depicted in the graph. For the final configuration, instead, the optimization tool has modified the blade design, avoiding any possible resonances, both for the first EO and for NPF.

The original and optimized overall performance is summarized in Table 4.

Table 4 Original and optimized overall performance for radial inflow turbine

	Original	Optimized
$\dot{m}$ [kg/s]	0.907	0.75
η_{t-t} [–]	0.872	0.927
Power [kW]	250.24	246.17
u/c_0	0.655	0.651
Stress usage factor [–]	2.54	0.98
Resonance 4OE	Yes	No
Resonance NPF	Yes	No

10. Conclusion

In this work, a multidisciplinary optimization procedure, partially based on an open source software, has been described and discussed. The aim of the work was to illustrate a multidisciplinary procedure capable of increasing aerodynamic efficiency guaranteeing mechanical safety for high speed radial gas turbines and centrifugal compressors. The paper illustrates the coupling between widely used CFD commercial software and open source tools for mesh generation and mechanical analysis. The coupling has been obtained via in-house developed Python and FORTRAN scripts suited for the current application. Through this integrated design approach, starting from a preliminary 1D design, the following goals have been achieved:

- higher efficiency;
- Von Mises stress field below the allowable limits, defined as a function of temperature for the turbine case;
- Free from resonance behaviour of the two impellers, in the speed operating regime, for the sources of excitation considered.

The efficiency enhancement achieved for the singular components enables to obtain a theoretical overall efficiency increase of around 6%, bringing the state of the art overall efficiency from a starting value of 30% up to an optimized value of about 36%, close to the reciprocating engines one. At this step, the results appear very promising. However, further thorough analyses have to be carried out before passing at the detailed design and prototype manufacturing.

The planned analyses concern:

- off design aero-thermomechanical simulations in order to estimate the system performance over the complete range of operating conditions;
- advanced, high resolution simulations to overcome possible turbulence model limitations and tip clearance effects on design point aerodynamic performance;
- unsteady rotor-stator aerodynamic interaction simulations to assess unsteady aerodynamic and mechanical effect on the system performance over the complete range of operating conditions.

References

[1] Mueller L., Alsalihi Z., Verstraete T. Multidisciplinary Optimization of Turbocharger Radial Turbine. Journal of Turbomachinery, 2013, 135(2): 021022.

[2] Verstraete T., Alsalihi Z., Van den Braembussche R. Multidisciplinary Optimization of a Radial Compressor for Micro gas Turbine Applications. Journal of Turbomachinery, 2010, 132(3): 031004.

[3] Barsi D., Perrone A., Ratto L., Simoni D., Zunino P. Radial inflow turbine design through Multidisciplinary optimization technique. ASME Turbo Expo 2015: Turbine Technical Conference and Exposition GT2015 Montreal, Canada, June 15–19: 2015.

[4] Perrone A., Ratto L., Ricci G., Satta F., Zunino P. Multi-Disciplinary Optimization of a Centrifugal Compressor for Micro-Turbine Applications. ASME Turbo Expo 2016: Turbine Technical Conference and Exposition GT2016, Seul, South Corea, June 13–17, 2016.

[5] Zunino P. Advanced design of micro-gas-turbines for distributed co-generation, Invited Lecture at Next Turbine, Shanghai, China, 2015.

[6] GTcycle, https://github.com/ampsolutions/gtcycle (accessed 2 February 2017).

[7] Cumpsty N. A.. Compressor aerodynamics, Longman Scientific & Technical, England, 1989.

[8] Rothe P. H., Johnston J. P. Effects of system rotation on the performance of two-dimensional diffusers, Journal of Fluids Engineering, 1976, 98.3: 422–429.

[9] Moore J. A Wake and an Eddy in a Rotating, Radial-Flow Passage - Part 1: Experimental Observations, Part 2, Flow Model. Journal of Engineering for Power, 1973, 95(3): 205–219.

[10] Casey M., Gersbach F., Robinson C. An optimization technique for radial compressor impellers. ASME Turbo Expo 2008, Berlin, Germany, June 9–13, 2008: 2401–2411.

[11] Eckardt, D. Detailed flow investigations within a high-speed centrifugal compressor impeller. Journal of Fluids Engineering, 1976, 98(3): 390–399.

[12] Krain H. Swirling impeller flow. Journal of Turbomachinery, 1988, 110.1: 122–128.

[13] Wang Y., Wang K., Tong Z., Lin F., Nie C., Engeda A. Design and optimization of a single stage centrifugal compressor for a solar dish-Brayton system. Journal of Thermal Science, 2013, 22(5): 404–412.

[14] Whitfield A, Baines N. C.. Design of radial turbomachines, Longman Scientific & Technical, 1990.

[15] Rohlik H. E., Radial-inflow turbines, Glassmann A J (Editor). Turbine design and application, 1975, NASA SP 290, 3.

[16] Chen H., Baines N. C. Analytical optimization design of radial and mixed flow turbines. Proceedings of the Institution of Mechanical Engineers, Part A: Journal of Power and Energy, 1992, 206 (3): 177–187.

[17] Cox G. D., Fischer C., Casey M. V. The application of through flow optimisation to the design of radial and mixed flow turbines. 9th International Conference on Turbochargers and Turbocharging, 2010, London: 217–226.

[18] NUMECA, User manuals. Academic R&D license 2017.

[19] Hirsch C., Lacor C., Rizzi A., Eliasson P., Lindblad I., Haeuser J. A multiblock/multigrid code for the efficient solution of complex 3D Navier-Stokes flows. Aerothermodynamics for Space Vehicles 1, 1991, SEE N92-14973 06-02: 415–420.

[20] Bourgeois J.A., Martinuzzi R.J., Savory E., Zhang C., Roberts D.A. Assessment of Turbulence Model Predictions for an Aero-Engine Centrifugal Compressor. ASME. Journal of Turbomachinery, 2011, 133(1): 011025.

[21] Mangani L., Casartelli E., Mauri S. Assessment of Various Turbulence Models in a High Pressure Ratio Centrifugal Compressor With an Object Oriented CFD Code. ASME. Journal of Turbomachinery, 2012, 134(6): 061033

[22] Van den Braembussche R.A., Prinsier J., Di Sante A. Experimental and numerical investigation of the flow in rotating diverging channels. Journal of Thermal Science, 2010, 19(2): 115–119.

[23] Geuzaine C., Remacle J. F. Gmsh: a three-dimensional finite element mesh generator with built-in pre- and post-processing facilities. International Journal for Numerical Methods in Engineering, 2009, 79(11): 1309–1331.

[24] CALCULIX, A Free Software Three-Dimensional Structural Finite Element Program, https://www.calculix.de (accessed 23 November 2016).